

# PHYSICAL REVIEW LETTERS

VOLUME 8

APRIL 15, 1962

NUMBER 8

## TRAPPING AND PROLONGED CONFINEMENT OF AN ENERGETIC DEUTERIUM PLASMA IN A STATIC CUSPED MAGNETIC FIELD\*

John E. Osher

Los Alamos Scientific Laboratory, University of California, Los Alamos, New Mexico

(Received March 19, 1962)

In this experiment an energetic plasma jet is injected axially into a bi-conical cusped magnetic bottle (picket fence)<sup>1</sup> to test the entropy trapping principle,<sup>2</sup> and to study confinement.<sup>3</sup> Neutrons and soft x rays are observed<sup>4</sup> in a prompt burst followed by initial fluctuations which then settle down to a smooth exponential tail with an average  $1/e$  decay time constant  $\tau$  of  $360 \mu\text{sec}$  at the limiting magnetic field of 6 kgauss. Neutrons can still be detected at 5 times background 5 milliseconds after injection. The total neutron yield in the tail reaches  $\sim 2 \times 10^6$ .

Previous studies have reported<sup>5-7</sup> high- $\beta$  ( $= 8\pi nKT/B^2$ ) trapping, in cusped systems, of plasmas with ion energies of  $\lesssim 150 \text{ eV}$ , diamagnetic signal decay times of  $\lesssim 30 \mu\text{sec}$ , and low- $\beta$  confinement times<sup>8</sup>  $\lesssim 200 \mu\text{sec}$ . Other experiments have described some degree of success with low- $\beta$  plasma trapping<sup>9</sup> in cusped fields or high- $\beta$  trapping<sup>10</sup> in mirror magnetic fields.

The experimental arrangement is shown in Fig. 1. Injection is from a coaxial hydromagnetic gun of the pulsed-gas type<sup>11</sup> operating in a new low-gas-density regime<sup>12</sup> which gives increased deu-

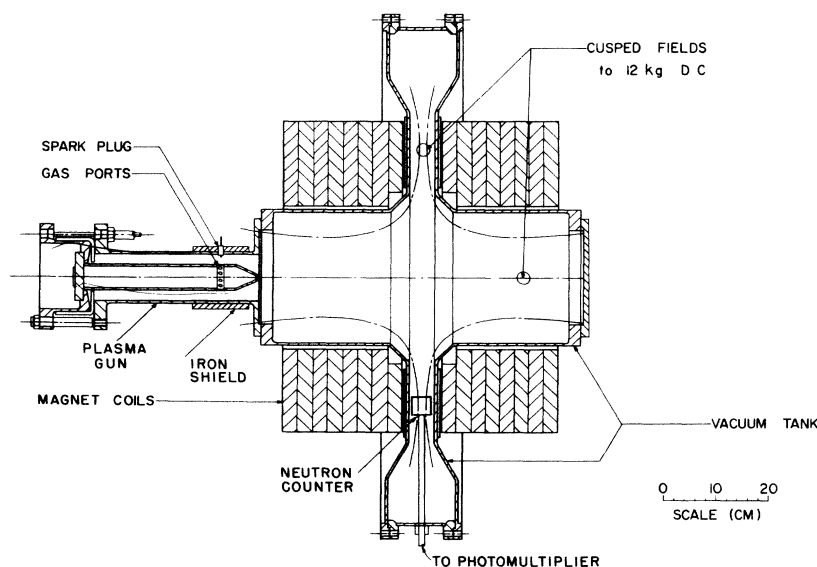


FIG. 1. A schematic drawing of the coaxial plasma gun and the picket fence magnet geometry.

teron velocities.

The Mark IIB picket fence has peak cusped magnetic fields of up to 12 kgauss located about 25 cm from the field zero. The stainless steel vacuum vessel is bulged out beyond the ring cusp region with the purpose of delaying the return (to the central confinement region) of cold material formed from the escaping energetic plasma.

The instrumentation used is as follows: Fast neutron counters consisting of plastic scintillator photomultiplier combinations are used to study the neutron time history, with data generally recorded by a counter located at the ring cusp as shown in Fig. 1. In view of the long confinement times we report, special precautions were taken to evaluate the signal tail generated by a pulse of neutrons reflected from the walls of the room and then observed as slow ( $n, \gamma$ ) captures in the plastic scintillator. For this, a pulsed neutron generator of known characteristics was placed in the interior of the picket fence vacuum chamber adjacent to the ring cusp counter. An exponential decay tail was detected with a  $\tau$  of  $\sim 100 \mu\text{sec}$  but with an integrated signal tail amounting to only 3% of the prompt pulse, which is negligible compared to the signal tails described below. Absolute neutron yields are measured with a standardized slow-neutron silver activation counter. X rays are detected by a thin scintillator located behind a  $3.4\text{-mg/cm}^2$  Al foil in a collimated channel aimed across the axial cusp region of the picket fence. A momentum analysis of the ions escaping from the ring cusp is made using a magnetic analyzer.

The injected  $D^+$  energy spectrum measured by magnetic analysis with time-of-flight discrimination at a point two meters from the gun muzzle (picket fence field turned off) is shown in Fig. 3(a). The total plasma jet consists of approximately  $5 \times 10^{16}$   $D^+$  ions with a mean energy  $\bar{E} = 13$  keV, where

$$\bar{E} = \int_0^\infty E \frac{dn}{dE} dE / \int_0^\infty \frac{dn}{dE} dE,$$

plus a small  $D_2^+$  component, and traces of  $D_3^+$  and impurities. This plasma is directed axially into the entrance cusp of the picket fence at a density of  $3 \times 10^{13}/\text{cm}^2$ . The electron energy distribution in the plasma jet has not yet been measured, but it is assumed to consist mainly of electrons of a few electron volts, though a prompt burst ( $\sim 5 \mu\text{sec}$  duration) of  $\sim 13\text{-keV}$  x rays indicates some energetic electrons. The plasma jet

from the gun appears to stagnate in the entrance cusp for fields  $> 4.2$  kgauss. As a result, the data from 4.2 kgauss to 6.0 kgauss (ring and exit cusp fields) are obtained by use of a magnetic shield around the gun muzzle, as shown in Fig. 1, to decrease the axial magnetic field in the entrance cusp region.

On injection we see the familiar short-lived, fairly high  $\beta$ , diamagnetic signal and also a prompt 1- to 5- $\mu\text{sec}$  neutron signal containing  $N_p$  neutrons as evaluated by the prompt rise in the integrated neutron signal as shown in Fig. 2. Following this, there is a tail containing  $N_t$  neutrons.

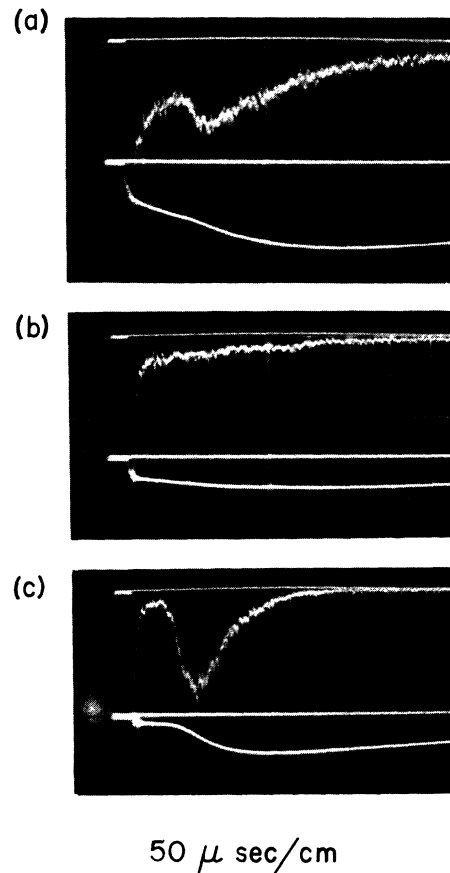


FIG. 2. Three sets of neutron signals ( $50 \mu\text{sec/cm}$ ) from the ring cusp counter at cusp fields of 4.9 kgauss. The neutron signal in each upper trace was smoothed by a  $0.15\text{-}\mu\text{sec}$  integrator for clarity. The lower trace shows the corresponding signal when integrated with a  $510\text{-}\mu\text{sec}$  time constant. These photographs are examples of (a) a signal hump followed by a smooth decay, (b) a smooth transition from the prompt pulse to the long tail, and (c) a reduced containment time produced by probe interference.

Plasma trapping and confinement are measured from the amplitude and time history of the neutron tail. For cusped fields of 0 to 2 kgauss the ratio  $N_t/N_p$  remains a constant  $\approx 0.03$  as expected from only the  $(n, \gamma)$  tail and no trapping. For cusped fields of 2 to 6 kgauss the traces generally show a neutron tail with ratios of  $N_t/N_p$  ranging from 0.1 to 5.0, indicating efficient trapping. A typical set of neutron signals from the ring cusp counter is shown in Fig. 2 for cusp fields of 4.9 kgauss. The neutron tail can be a smooth exponential, but more often it shows a moderate hump (not yet understood)  $\sim 50$  to  $150 \mu\text{sec}$  after injection and then the signal smooths out to an exponential tail. The average lifetime obtained from these exponential tails increases rapidly with magnetic field ( $\tau \propto B^3$ ) from  $\tau \sim 10 \mu\text{sec}$  at 2 kgauss to  $\tau = 360 \mu\text{sec}$  at 6 kgauss. A neutron counter located outside the exit cusp shows a similar tail, but with a relatively larger  $N_p$  pulse and smaller  $N_t/N_p$  ratios. The soft x-ray detector shows a prompt x-ray pulse, followed by signal fluctuations that smooth out at about  $50 \mu\text{sec}$ , and then follows the same shape and slope ( $\tau$ ) as the neutron signals within experimental error.

The energy spectrum of ions ( $D^+$  assumed to dominate) escaping from the ring cusp (4.9-kgauss field) 100  $\mu\text{sec}$  and 300  $\mu\text{sec}$  after plasma injection is shown in Fig. 3(b). We see that the mean energy is degraded down from 13 keV on injection to  $\sim 5$  keV at these times, with about 5% of the ions having energies  $> 20$  keV. Assuming that the loss spectrum is a representative sample of the trapped plasma, one can utilize the high-energy component of the spectrum and the observed average total neutron tail yield of  $\sim 8 \times 10^5$  (average total neutron yield  $\sim 3 \times 10^6$ ) to calculate a total average trapped density of at least  $2 \times 10^{12}$  deuterons/cm<sup>3</sup> (with an average  $\bar{E} \approx 5$  keV) in a volume of about  $10^4$  cm<sup>3</sup>. The plasma radial dimensions are inferred by the onset of probe interference at  $\sim 15$  to 17 cm radius at the radial and exit cusps. Voltage probe measurements also indicate an  $\sim 2$ -cm sheath at about 15 cm radius and qualitatively place the confined region in a negative potential well of the order 1 kv. X-ray absorption data (taken at 3.2 kgauss) give a good fit to a 1.4-keV temperature, though long relaxation times probably preclude a true equilibrium. In addition, preliminary measurements with a pinhole nuclear emulsion camera (6.85-

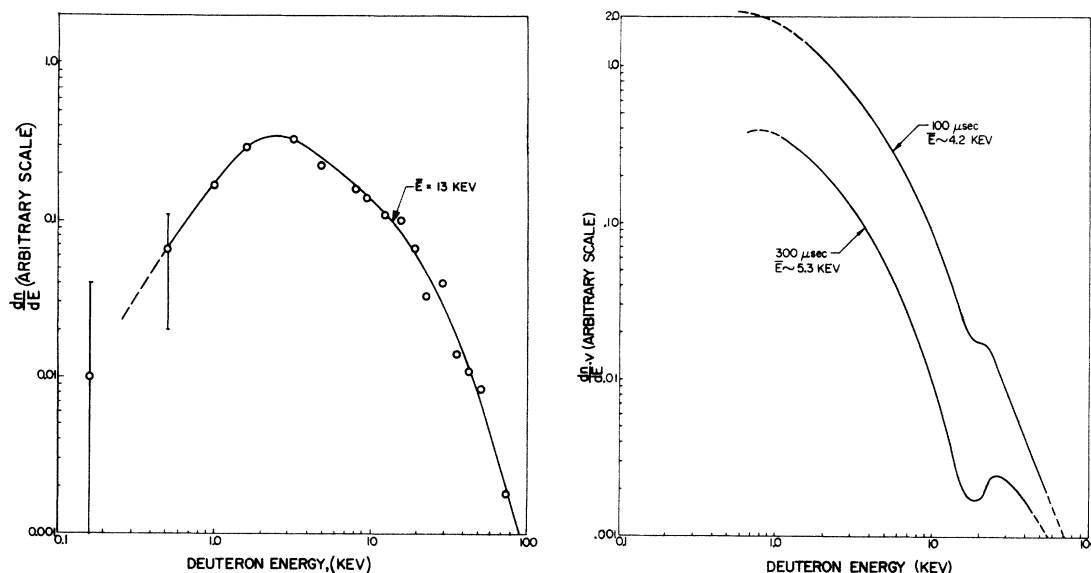


FIG. 3. (a) The  $D^+$  ion energy spectrum of the plasma injected from the coaxial plasma gun, where  $dN/dE$  represents the total number of  $D^+$  ions per unit energy interval in arbitrary units (measurements made with picket fence field off). (b) Preliminary measurements of the  $D^+$  ion energy spectrum escaping out of the ring cusp 100  $\mu\text{sec}$  and 300  $\mu\text{sec}$  after injection (4.9-kgauss ring cusp field). The ordinate  $dN/dE$  times velocity is the total number of  $D^+$  ions per unit energy interval per unit time in arbitrary units. Note the depletion of  $D^+$  ions near 17 keV, presumably from charge exchange losses.

mg/cm<sup>2</sup> Al window) indicate (1) a strong volume x-ray source and (2) an average *d*-D volume yield (of 3.02-Mev protons)  $< 2 \times 10^5$ . Fast-neutron counter measurements are consistent with the major *d*-D neutron yield occurring on the walls just outside the cusped fields.

The confined plasma is sensitive to external perturbations; for example, the trapped signal amplitude  $N_t$  can be markedly increased by a small increase or skew in the exit cusp magnetic field or by a decrease in the entrance cusp field. As might be expected, the confinement time is curtailed by insertion of a probe or injection of extra D<sub>2</sub> gas. The latter includes two special cases: (1) Trapping ceases for pressures  $> 7 \times 10^{-5}$  mm of Hg, and (2) for pulsed neutral gas injection or static background D<sub>2</sub> pressure  $\leq 5 \times 10^{-5}$  mm of Hg, the neutron traces first show a large hump with a shortened lifetime and then often the slope recovers to the  $\tau$  of a good vacuum ( $2 \times 10^{-6}$  mm of Hg).

The long confinement time with the measured high ion energies represents an interesting regime which seems critically related to improved gun performance. A careful search of possible sources of error such as the following has been made: (1) large space potentials to accelerate the deuterons (the potential has been measured and is small), and (2) late production of energetic ions by the gun (inconsistent with gun behavior and other measurements).

The observed plasma lifetimes are about an order of magnitude larger than the simple theoretical expression,  $\tau = 10^{-10} R^2 B / T_{\text{keV}}$ , due to Berkowitz *et al.*,<sup>13</sup> for  $\beta = 1$  confinement in a cusped system filled to maximum capacity. The theoretical lifetimes calculated for single-particle orbits (closer to the low- $\beta$  conditions of this experiment) predict<sup>14,15</sup> similar short confinement times for the nonadiabatic region near the field zero. The relatively large size of the D<sup>+</sup> orbits in the Mark IIb picket fence places the entire volume in the nonadiabatic confinement region. This leaves us with the discrepancy of longer observed lifetimes than theory would predict. A preliminary model proposed here to explain the long ion confinement time is to consider the electrons as being trapped in an adiabatic (for them) cusped field. These electrons form a negative potential well (as observed) which reduces the nonadiabatic ion loss rate through the cusps. The well depth would adjust itself until the modified ion loss rate equals the nonadiabatic electron losses such as Coulomb collisions (i.e.,  $\tau_{\text{ion}}$

$$\sim \tau_{ee} = 3 \times 10^8 E_{e, \text{keV}}^{3/2} / n_e).$$

Another problem is the expected loss of energetic ions through charge exchange with neutral gases. The observed 360- $\mu$ sec  $\tau$  can be accommodated within known cross sections for background pressures  $\leq 2 \times 10^{-6}$  mm of Hg or neutron production by deuterons of energies  $\geq 50$  keV, providing one assumes that there is no extra influx of neutral gas from the gun. However, this problem becomes acute when one considers the confinement data at static (or injected) D<sub>2</sub> pressures of up to  $5 \times 10^{-5}$  mm of Hg, where the large  $N_t$  amplitude traces show an initially shortened lifetime which often recovers to a  $\tau$  of up to 360  $\mu$ sec (its average good-vacuum value). To remain consistent with charge exchange, we require either deuterons  $> 250$  keV or at least 98% ionization of neutrals (at the probably 30 to 50 keV deuteron energy responsible for the neutron yield). From the measured deuteron spectrum and the physical size of the Mark IIb chamber (which excludes orbits of  $E > 100$  keV), we seem forced to the conclusion that classical "burnout" has occurred.<sup>16</sup>

The author acknowledges with gratitude the contributions of J. L. Tuck in proposing this experiment and the "bicycle tire" construction of the picket fence vacuum chamber, and also the contributions of J. A. Phillips, D. C. Hagerman, and many others throughout this experiment.

---

\*Work performed under the auspices of the U. S. Atomic Energy Commission.

<sup>1</sup>J. L. Tuck, Washington Report No. 184, 1954 (unpublished), p. 77; H. Grad, Washington Report No. 289, 1955 (unpublished), p. 115.

<sup>2</sup>J. L. Tuck, Phys. Rev. Letters **3**, 313 (1959).

<sup>3</sup>J. Berkowitz, H. Grad, and H. Rubin, Proceedings of the Second United Nations Conference on the Peaceful Uses of Atomic Energy, Geneva, 1958 (United Nations, Geneva, 1959), Vol. 31, p. 177.

<sup>4</sup>J. E. Osher, Bull. Am. Phys. Soc. **7**, 143 (1962).

<sup>5</sup>D. C. Hagerman and J. E. Osher, Phys. Fluids **4**, 905 (1961).

<sup>6</sup>S. Yu. Lukyanov and I. M. Podgoryni, Zhur. Eksp. i Teoret. Fiz. **37**, 27 (1959) [translation: Soviet Phys. - JETP **10**, 18 (1960)].

<sup>7</sup>F. R. Scott and H. G. Voorhies, Phys. Fluids **4**, 600 (1961).

<sup>8</sup>D. C. Hagerman, Conference on Plasma Physics and Controlled Nuclear Fusion Research, Salzburg, 1961 (unpublished), Paper No. CN-10/154.

<sup>9</sup>F. H. Coensgen, A. E. Sherman, W. E. Nexsen, and W. F. Cummins, Phys. Fluids **3**, 764 (1960).

<sup>10</sup>F. R. Scott and O. C. Eldridge, Jr., Phys. Fluids **4**, 1558 (1961).

- <sup>11</sup>J. Marshall, *Phys. Fluids* **3**, 134 (1960).  
<sup>12</sup>J. E. Osher and D. C. Hagerman, *Bull. Am. Phys. Soc.* **5**, 350 (1960).  
<sup>13</sup>J. Berkowitz, K. O. Friedrichs, H. Goertzel, H. Grad, J. Killeen, and E. Rubin, reference 3, p. 171.  
<sup>14</sup>H. Grad, Atomic Energy Commission Report NYO-

- 9496, 1961 (unpublished).  
<sup>15</sup>E. P. Gray and I. M. Miller, Applied Physics Laboratory, Johns Hopkins University, Silver Springs, Maryland, Report CPR-010, 1961 (unpublished).  
<sup>16</sup>C. F. Barnett, P. R. Bell, J. S. Luce, E. D. Shipley, and A. Simon, reference 3, p. 298.

## MEASUREMENT OF THE HALL EFFECT IN METAL-FREE PHTHALOCYANINE CRYSTALS

George H. Heilmeyer and George Warfield  
 Princeton University, Princeton, New Jersey

and

Sol E. Harrison  
 RCA Laboratories, Princeton, New Jersey  
 (Received March 7, 1962)

The very low conductivity of organic semiconductors makes it extremely difficult to measure a Hall voltage in these materials. If one uses sensitive ac methods for detection, the signal voltage is usually comparable to the noise voltage. Previous attempts at Hall measurements on organic semiconductor crystals and films<sup>1-3</sup> have succeeded only in establishing an upper limit for carrier concentration and mobility. It is the purpose of this note to describe our techniques and results for Hall measurements on single crystals of metal-free phthalocyanine. This is believed to be the first Hall measurement ever reported on organic semiconductor crystalline solids.

The crystals tend to grow as needles and are extremely brittle, making them difficult to cut and impossible to work mechanically. Likely specimens<sup>4</sup> were selected carefully and had typical dimensions of: length, 5 mm; width, 0.5 mm; thickness, 0.3 mm. They were found to contain the following metallic impurities in parts per million: Cu, 200-2000; Na, 1-10;

Ca, 1-10; Fe, 6-60; Si, 0.1-1; Mg, 3-30; Al, <1. No measure of the organic impurities is available at this time. Silver paste was found to make Ohmic contact to this material for fields 15 volts/cm to 10<sup>3</sup> volts/cm.

The schematic diagram of the experimental setup is shown in Fig. 1. The measurement technique consisted of recording the output of the electrometer across the Hall probes as a function of time, with the magnetic field on, off, and reversed. A typical result with field in a specific direction is shown in Fig. 2. The data were integrated using a planimeter to eliminate the effects of noise. The results of measurements on several samples are given in Table I, where it has been assumed in the calculation of the Hall coefficient, mobility, and carrier concentration that only one type of carrier is mobile, a band model is applicable, and the conductivity is isotropic.<sup>5</sup>

Careful thermal-probe measurements confirmed that the sign of the carriers in these crystals was negative.

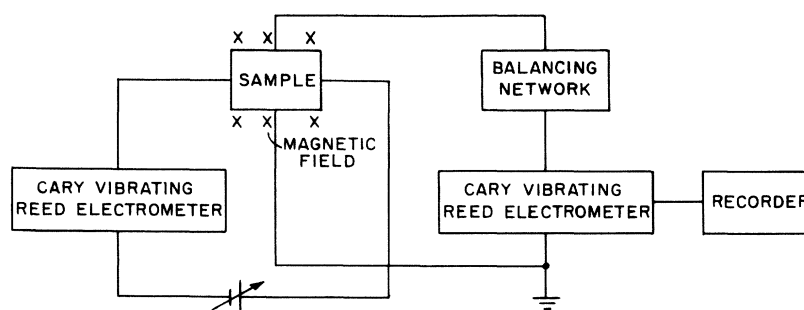


FIG. 1. Schematic diagram of Hall measurement equipment.

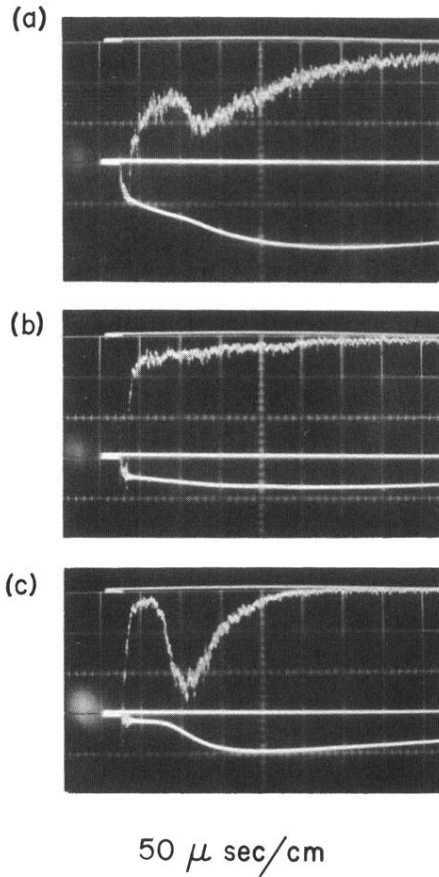


FIG. 2. Three sets of neutron signals ( $50 \mu\text{sec/cm}$ ) from the ring cusp counter at cusp fields of 4.9 kgauss. The neutron signal in each upper trace was smoothed by a  $0.15\text{-}\mu\text{sec}$  integrator for clarity. The lower trace shows the corresponding signal when integrated with a  $510\text{-}\mu\text{sec}$  time constant. These photographs are examples of (a) a signal hump followed by a smooth decay, (b) a smooth transition from the prompt pulse to the long tail, and (c) a reduced containment time produced by probe interference.